

Singularities you might not be familiar with

Andrzej Krasiński

N. Copernicus Astronomical Center, Polish Academy of Sciences

Contents

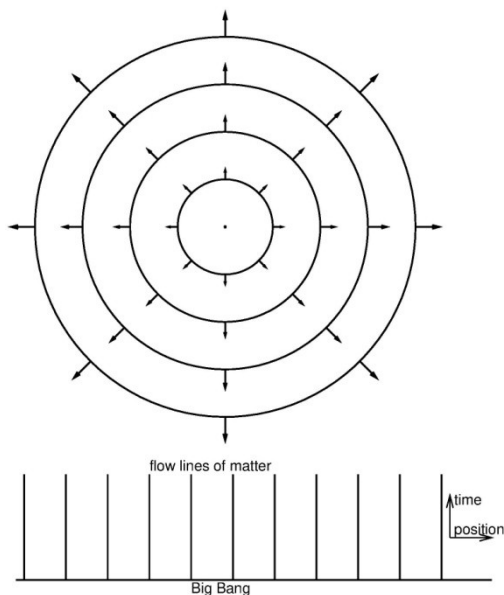
| | | |
|----------|--|-----------|
| 1 | Motivation | 2 |
| 2 | Spherically symmetric inhomogeneous models | 3 |
| 3 | The Lemaître – Tolman model | 6 |
| 4 | Applications of of the L–T model with nonconstant Big Bang | 13 |
| 4.1 | Example 1: Explaining away the accelerated expansion of the Universe . . . | 13 |
| 4.2 | Example 2: Modelling the gamma-ray bursts (GRBs) | 18 |
| 5 | How would a shell crossing in an L–T model be seen by observers? | 25 |
| 6 | Expression of hope | 28 |
| 7 | References | 29 |
| 8 | Appendix: The quasi-spherical Szekeres models | 34 |
| 9 | Blueshifts in quasi-spherical Szekeres models | 37 |

1. Motivation

A great body of literature exists on singularities in general relativity (e. g. [1, 2]).

But explicit examples in exact solutions of Einstein's equations are not many.

The only widely known cosmological singularity is that in the Robertson - Walker models [3-5], and it is extremely simple.



In comoving coordinates, all matter particles emerge from the Big Bang simultaneously.

The only physical implication of this singularity is high mass-density of matter at early times.

I will show examples of singularities in models less symmetric than R-W.

2. Spherically symmetric inhomogeneous models

The R-W models are derived from Einstein's equations by assuming spherical symmetry and spatial homogeneity.

The simplest generalisations are obtained by dropping one or the other of these assumptions.

Dropping the assumption of spherical symmetry one obtains the spatially homogeneous Bianchi-type models.

This class is already well-investigated, and still in good hands, so I will not discuss it here.

A different generalisation results when the assumption of homogeneity is dropped, while that of spherical symmetry is retained.

The most general spherically symmetric metric is:

$$d s^2 = e^{C(t, r)} dt^2 - e^{A(t, r)} dr^2 - R^2(t, r) (d\vartheta^2 + \sin^2\vartheta d\varphi^2). \quad (2.1)$$

Assuming a perfect fluid source in the Einstein equations, the coordinates of (2.1) may be made comoving without loss of generality:

$$u^\alpha = e^{-C/2} \delta^\alpha_0. \quad (2.2)$$

We will further assume that the source is dust ($p = 0$). Then $C = C(t)$ and a simple transformation of t results in $C = 0$.

$$d s^2 = dt^2 - e^{A(t,r)} dr^2 - R^2(t,r) (d\vartheta^2 + \sin^2\vartheta d\varphi^2). \quad (2.1)$$

$$u^\alpha = \delta^\alpha_0. \quad (2.2)$$

$$p = 0$$

With (2.1) – (2.2) the Einstein equations become (we allow $\Lambda \neq 0$ for a while):

$$\begin{aligned} G^0_0 &= \frac{R_{,t}^2}{R^2} + \frac{A_{,t} R_{,t}}{R} - e^{-A} \left(2 \frac{R_{,rr}}{R} + \frac{R_{,r}^2}{R^2} - \frac{A_{,r} R_{,r}}{R} \right) + \frac{1}{R^2} \\ &= \kappa\rho - \Lambda, \end{aligned} \quad (2.3)$$

$$G^1_0 = e^{-A} \left(2 \frac{R_{,tr}}{R} - \frac{A_{,t} R_{,r}}{R} \right) = 0, \quad (2.4)$$

$$G^1_1 = 2 \frac{R_{,tt}}{R} + \frac{R_{,t}^2}{R^2} - e^{-A} \frac{R_{,r}^2}{R^2} + \frac{1}{R^2} = -\Lambda, \quad (2.5)$$

$$\begin{aligned} G^2_2 &= G^3_3 = \\ &= \frac{R_{,tt}}{R} + \frac{A_{,t} R_{,t}}{2R} + \frac{A_{,tt}}{2} + \frac{A_{,t}^2}{4} - e^{-A} \left(\frac{R_{,rr}}{R} - \frac{A_{,r} R_{,r}}{2R} \right) \\ &= -\Lambda. \end{aligned} \quad (2.6)$$

$$d s^2 = dt^2 - e^{A(t,r)} dr^2 - R^2(t,r) (d\vartheta^2 + \sin^2\vartheta d\varphi^2). \quad (2.1)$$

$$G^1_0 = e^{-A} \left(2 \frac{R_{,tr}}{R} - \frac{A_{,t} R_{,r}}{R} \right) = 0, \quad (2.4)$$

3. The Lemaître - Tolman (L-T) model

Equation $G^1_0 = 0$ (see above) can be written as follows:

$$\left(e^{-A/2} R_{,r} \right)_{,t} = 0. \quad (3.1)$$

One solution of this is $R_{,r} \equiv 0$. This leads to the model found by V. A. Ruban [6,7] which is a generalisation of Kantowski – Sachs. So far it has not been related to any observed object.

When $R_{,r} \neq 0$, eq. (3.1) leads to

$$e^A = \frac{R_{,r}^2}{1 + 2E(r)}, \quad (3.2)$$

where $E(r)$ is an arbitrary function.

$$ds^2 = dt^2 - e^{A(t,r)} dr^2 - R^2(t,r) (d\vartheta^2 + \sin^2\vartheta d\varphi^2). \quad (2.1)$$

$$e^A = \frac{R_{,r}^2}{1 + 2E(r)}, \quad (3.2)$$

With (3.2), excluding the case $R_{,t} = 0$ (which leads to the static Einstein model), the remaining Einstein equations are equivalent to the following two:

$$R_{,t}^2 = 2E(r) + \frac{2M(r)}{R} - \frac{1}{3}\Lambda R^2, \quad (3.3)$$

where $M(r)$ is one more arbitrary function, and:

$$\frac{8\pi G}{c^2} \rho = \frac{2M_{,r}}{R^2 R_{,r}}, \quad (3.4)$$

which defines the mass density. The final metric is

$$ds^2 = dt^2 - \frac{R_{,r}^2}{1 + 2E(r)} dr^2 - R^2(t,r) (d\vartheta^2 + \sin^2\vartheta d\varphi^2). \quad (3.5)$$

$$d s^2 = dt^2 - e^{A(t,r)} dr^2 - R^2(t,r) (d\vartheta^2 + \sin^2\vartheta d\varphi^2). \quad (2.1)$$

$$\frac{8\pi G}{c^2} \rho = \frac{2M_{,r}}{R^2 R_{,r}}, \quad (3.4)$$

The mass density becomes infinite where $R = 0 \neq M_{,r}$ and where $R_{,r} = 0 \neq M_{,r}$.

The first set is the **Big Bang**.

The second one is the **shell-crossing singularity**.

On it, the radial geodesic distance from $\{t_0, r_0, \vartheta_0, \varphi_0\}$ to $\{t_0, r_0 + dr, \vartheta_0, \varphi_0\}$ becomes zero \rightarrow shells having the r -coordinates r_0 and $r_0 + dr$ coincide.

$$ds^2 = dt^2 - \frac{R_{,r}^2}{1 + 2E(r)} dr^2 - R^2(t, r) (d\vartheta^2 + \sin^2 \vartheta d\varphi^2). \quad (3.5)$$

$$\frac{8\pi G}{c^2} \rho = \frac{2M_{,r}}{R^2 R_{,r}}, \quad (3.4)$$

The Big Bang is inevitable when $\Lambda = 0$.

Shell crossings do not exist when $M(r)$, $E(r)$ and $t_B(r)$ obey simple differential inequalities [8] ($dM/dr > 0$ and $dt_B/dr < 0$, one more depends on the sign of E).

In most applications of (3.5) one prefers to have no shell crossings.

I will return to them later.

The solution (3.5) was first found and interpreted by Lemaître in 1933 [9], then investigated by Tolman in 1934 [10] and Bondi in 1947 [11]. I will call it the Lemaître - Tolman (L-T) model.

[8] C. Hellaby, K. Lake, 1985.

$$R_{,t}^2 = 2E(r) + \frac{2M(r)}{R} - \frac{1}{3}\Lambda R^2, \quad (3.5)$$

When $\Lambda = 0$, the solutions of (3.5) can be found explicitly. They have the same algebraic form as the Friedmann solutions. For example, when $E(r) > 0$:

$$\begin{aligned} R(t, r) &= \frac{M}{2E}(\cosh \eta - 1), \\ \sinh \eta - \eta &= \frac{(2E)^{3/2}}{M} [t - t_B(r)]. \end{aligned} \quad (3.6)$$

The $t_B(r)$ is a third arbitrary function.

$t = t_B(r)$ is the Big Bang \rightarrow in general it occurs at different t for different r .

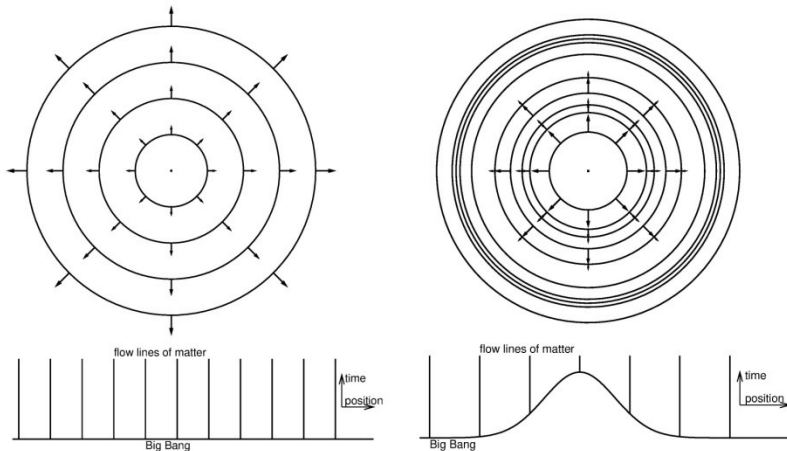
This means that in the natural cosmological synchronisation ***the particles of the cosmic medium have different ages at any given t .***

$$R_{,t}^2 = 2E(r) + \frac{2M(r)}{R} - \frac{1}{3}\Lambda R^2, \quad (3.5)$$

The Friedmann models result from (3.5) in the limit

$$M/r^3 = M_0, \quad 2E/r^2 = -k, \quad (3.7)$$

where M_0 , k and t_B are constant.



Expansion patterns in the Friedmann (left) and L-T models (right)

In the Friedmann models, the expansion velocity of each mass shell is proportional to its radius at any fixed time. The Big Bang is simultaneous in comoving coordinates.

In L-T models, the velocity of expansion of each shell is independent of its radius (the velocity distribution is an arbitrary function of r). The Big Bang is not simultaneous.

A shell crossing occurs when a mass shell of smaller radius expands too fast relative to a larger shell. Then, the smaller shell will catch up with the larger one, and they will stick together, creating a surface of infinite density.

$$R_{,t}{}^2 = 2E(r) + \frac{2M(r)}{R} - \frac{1}{3}\Lambda R^2, \quad (3.3)$$

$$\frac{8\pi G}{c^2}\rho = \frac{2M_{,r}}{R^2 R_{,r}}, \quad (3.4)$$

$$ds^2 = dt^2 - \frac{R_{,r}{}^2}{1 + 2E(r)} dr^2 - R^2(t, r) (d\vartheta^2 + \sin^2 \vartheta d\varphi^2). \quad (3.5)$$

In (3.3) E is seen to play the role of energy of the dust particle per unit mass.

At the same time, E measures the curvature of a 3-space of constant t (call it S_3). The scalar components of this curvature in an orthonormal tetrad are

$$R_{1212} = -\frac{E_{,R}}{R} = R_{1313}, \quad R_{2323} = -\frac{2E}{R^2} \quad (3.8)$$

→ $R_{ijkl} = 0$ when $E = 0$ and is constant when $E/R^2 = \text{const.}$

4. Applications of of the L-T model to cosmology

4.1. Example 1: Explaining away accelerated expansion of the Universe

The hypothesis of accelerated expansion of the Universe arose from observations of type Ia supernovae.

Their spatial distribution, inferred from comparing their observed luminosities with the calculated absolute luminosities, was inconsistent with the $\Lambda = 0$ Friedmann models.

Using other Friedmann models, the best fit to observations was when [12]:

spatial curvature index $k = 0$,

$\Omega_m = 32\%$ of the energy density comes from matter (visible or dark),

$\Omega_\Lambda = 68\%$ comes from "dark energy", a cosmological-constant-like entity.

[12] Planck 2013, part XVI

→ *The accelerated expansion is not an observed phenomenon.*

It is a model-dependent *element of interpretation* of observations.

It follows from the *assumption* that the model must be in the Friedmann class.

The example presented below [13-16] shows how the spurious accelerated expansion is reproduced in an L-T model using only $t_B(r)$.

This is the simplest method, but not the only one existing.

Example

The observer sits at $r = 0$ in an L-T model with $E/r^2 = \text{const}$ — the same as in the Friedmann models, and $t_B(r)$ defined via

$$D_A(z) = \frac{1}{(1+z)H_0} \int_0^z \frac{dz'}{\sqrt{\Omega_m(1+z')^3 + \Omega_\Lambda}} \quad (4.1)$$

(this relation holds in the now-standard Λ CDM model; D_A is the angular diameter distance to an object with redshift z).

The trick is that $H_0 = 67.1 \text{ km}/(\text{s}\times\text{Mpc})$, $\Omega_m = 0.32$ and $\Omega_\Lambda = 0.68$ are taken from observations [12], but

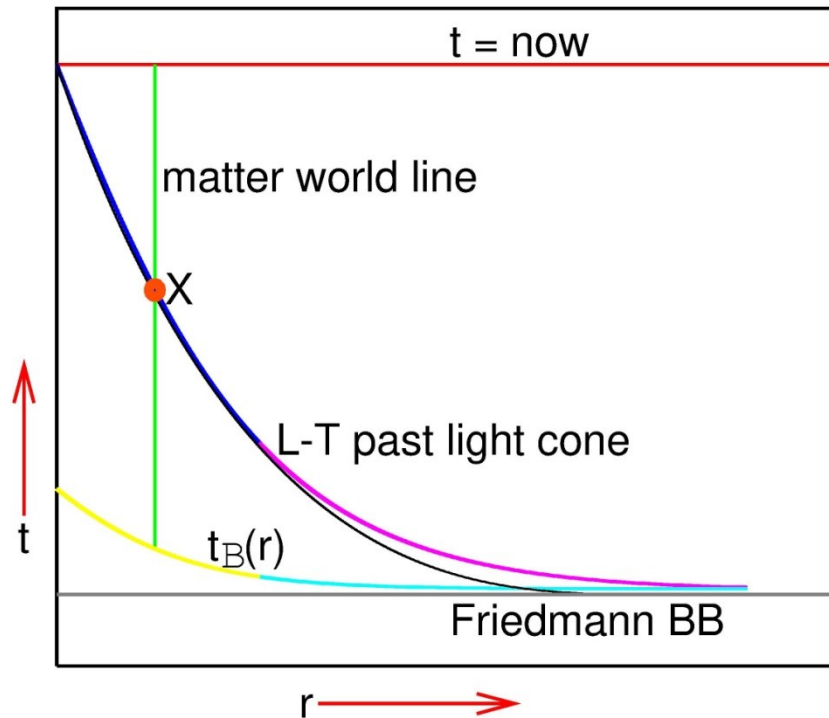
$$D_A(z) = R(t, r(z)) \Big|_{\text{on the past light cone}} \quad (4.2)$$

is taken from an L-T model.

Equation (4.1) can be numerically solved for $t_B(r)$ which is hidden in $R(t, r)$; the $r(z)$ relation is [11]:

$$\ln(1+z(r)) = \int_{r_{\text{obs}}}^{r_{\text{em}}} \frac{R_{,tr}(T(r), r)}{\sqrt{1+2E(r)}} dr. \quad (4.3)$$

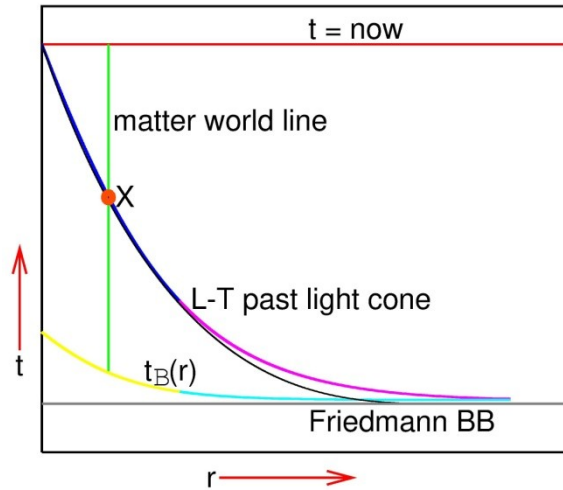
$$D_A(z) = \frac{1}{(1+z)H_0} \int_0^z \frac{dz'}{\sqrt{\Omega_m(1+z')^3 + \Omega_\Lambda}} \quad (4.1)$$



The $t(r)$ graph of the L-T past light cone that imitates accelerated expansion

The thin black curve is the past light cone of the Λ CDM model.

X = the instant when the world line of the observed particle intersects the observer's past light cone.



The L-T Big Bang occurs progressively later when the position of the observer is approached.

- The difference between the Friedmann age and the L-T age of the particle at X increases on approaching the observer.
- The expansion velocity at X is greater in L-T than in a Friedmann model with $\Lambda = 0 = k$, and the difference is increasing toward the observer.
- Instead of increasing with time, the expansion velocity *decreases with distance* even when $\Lambda = 0$.
- *Had we used an L-T model to interpret the observations, the "accelerated expansion" would not be implied, and there would be no need for "dark energy".*

4.2. Example 2: Modelling the gamma-ray bursts (GRBs)

In R-W models, a light ray emitted at the Big Bang reaches every observer with infinite *redshift*.

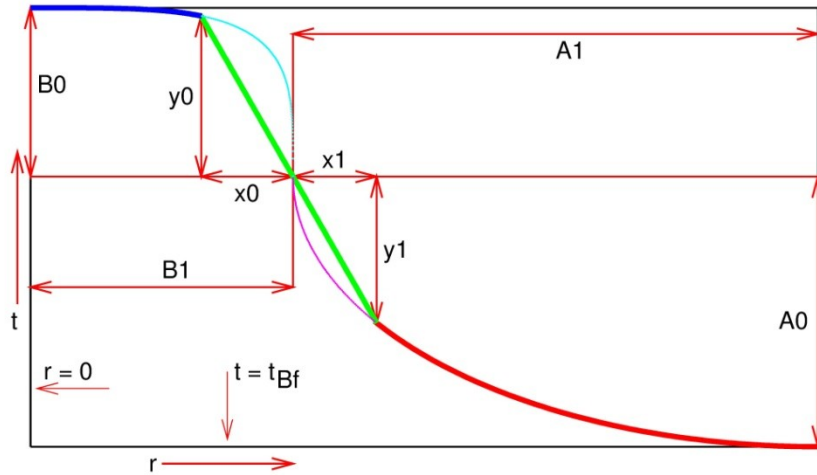
In an L-T model with nonconstant $t_B(r)$, a light ray emitted *radially* from the BB at a point where $dt_B/dr \neq 0$ reaches every observer with infinite *blueshift* ($z = -1$).

→ Rays emitted *close* to the BB can display strong blueshifts to present observers.

Blueshift is accumulated in a short time after the BB. Later-acquired redshift can overcompensate it. Whether this happens or not depends on the $t_B(r)$ profile.

The CMB rays were emitted at $\tau \approx 380\,000$ years after the BB [17].

With a suitable $t_B(r)$ profile, blueshift along a radial ray emitted at τ will survive the journey to the present observer, and z will be sufficiently near to -1 to account for the observed GRB energies [18].



This is a model of a single GRB source.

← A spherically symmetric hump is matched into a flat Big Bang profile.

The hump consists of two arcs connected by a straight line segment.

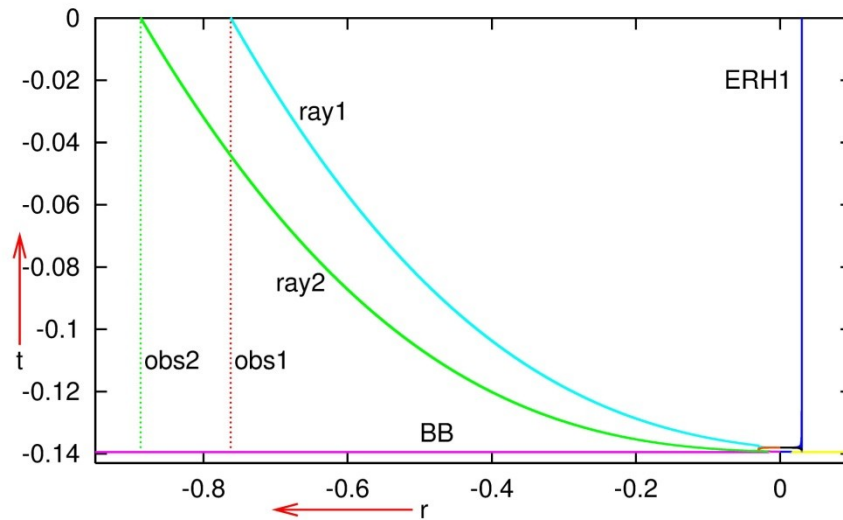
The upper-left arc is a segment of an ellipse-like 4-th degree curve:

$$\frac{r^4}{B_1^4} + \frac{(t - t_{Bf} - A_0)^4}{B_0^4} = 1, \quad (4.4)$$

The lower-right arc is a segment of an ellipse.

The straight segment passes through the point where the full arcs would be tangent to each other (it is there to avoid $dt_B/dr \rightarrow \infty$).

The profile has five parameters: A_0 , A_1 , B_0 , B_1 and x_0 .



The humps drawn in proportion to the age of the Universe and to the radius of the past light cone of the central observer

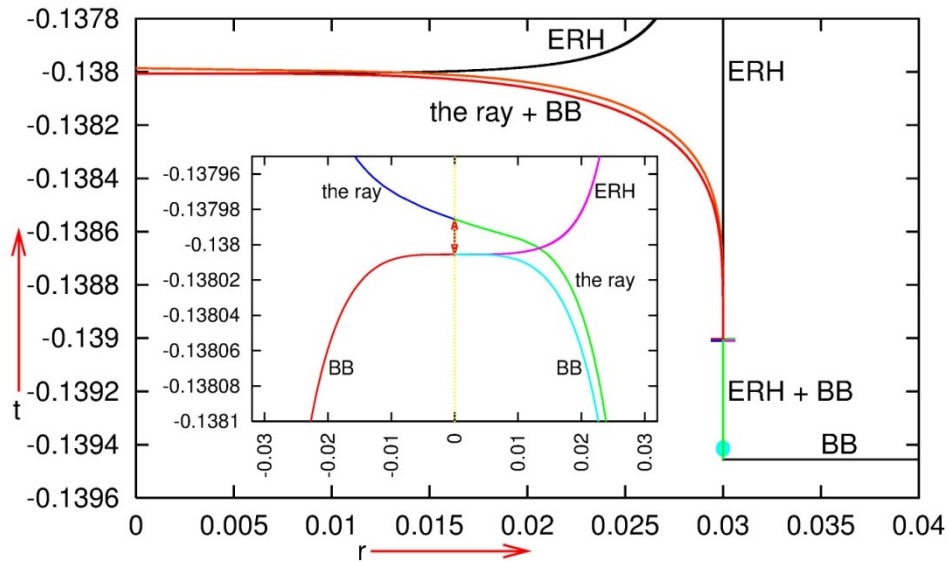
The higher hump models a source of a GRB of the highest observed energy.

The lower one models a source of the lowest observed energy.

It has the height $0.00089 \times (\text{the age of the Universe}) \approx 1.23 \times 10^7$ years,

and encompasses the mass $\approx 3.1 \times 10^6$ masses of our Galaxy

(calculated assuming the Λ CDM model parameters).

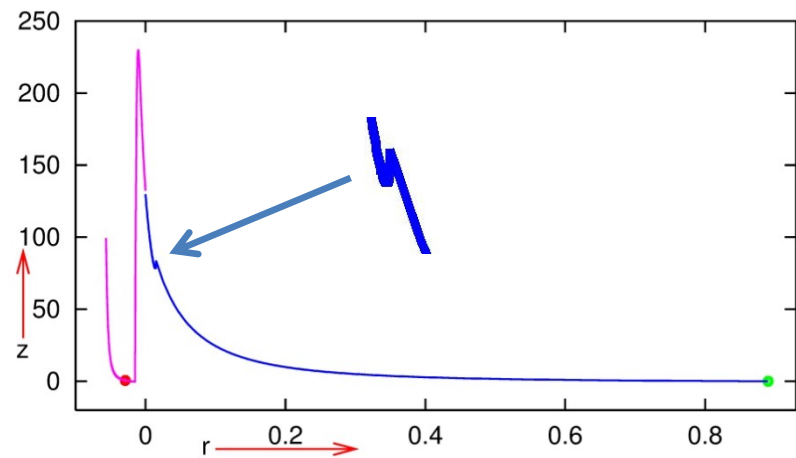
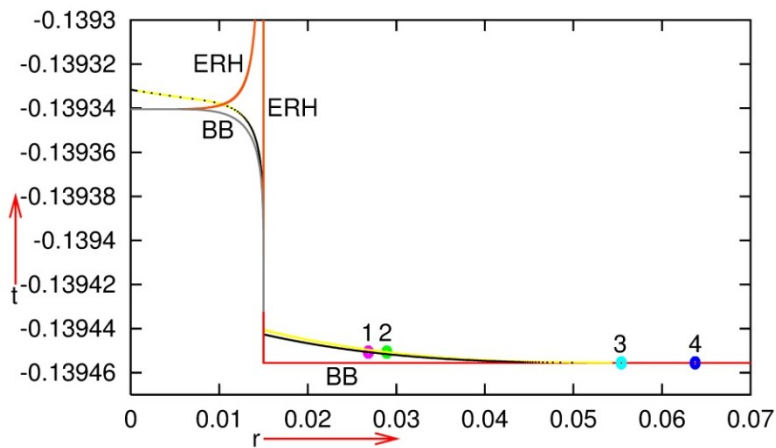


Magnified view on the blueshifted ray in a vicinity of the hump

Followed back in time, $z(r)$ initially increases and has a maximum at the first intersection with the ERH (*Extremum Redshift Hypersurface*).

Further into the past, $z(r)$ decreases (the ray locally acquires blueshift) up to the next intersection with the ERH.

The technical problem is to arrange the hump parameters so that the blueshift prevails over the redshift generated after the latest crossing of the ERH ($z \approx 10^3$) and moves the observed $1 + z$ into the range $[1.7 \times 10^{-5}, 2.5 \times 10^{-8}]$.



When local blueshifts are present, redshift fails to be a distance indicator.

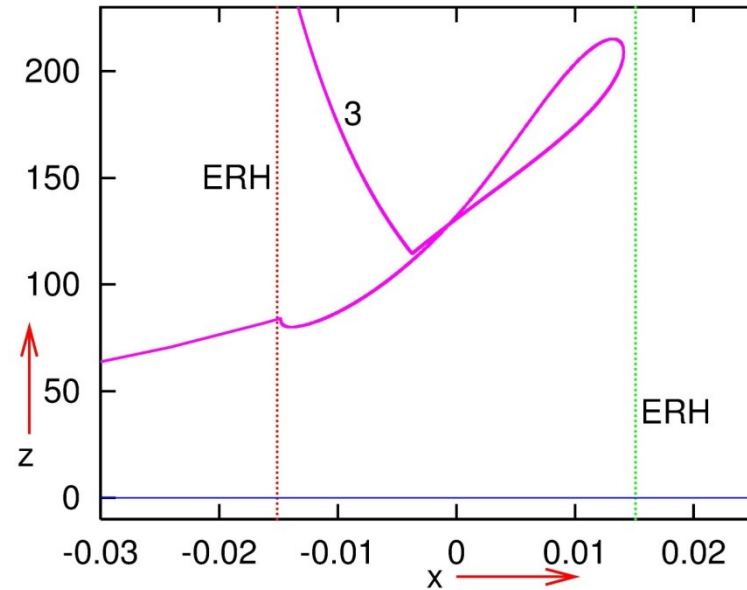
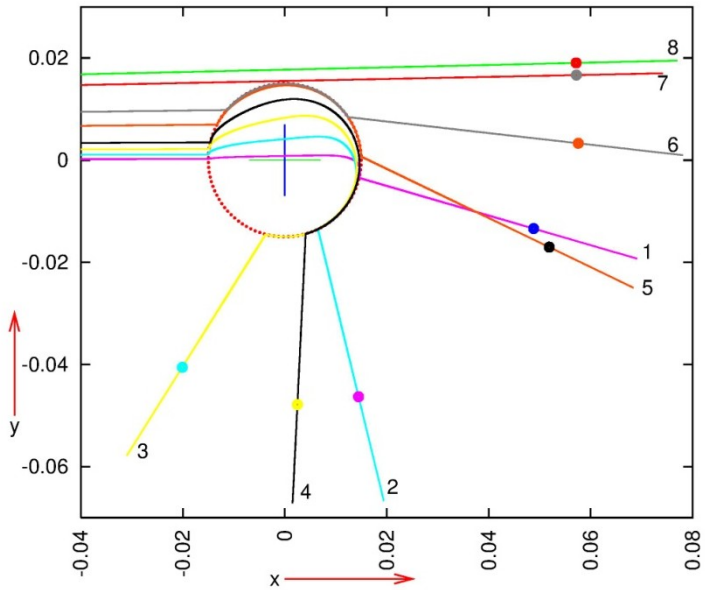
The right graph shows $z(r)$ seen by the observer (situated at the **green dot**) along the **yellow ray** depicted in the left graph.

The redshift first increases to the past, then decreases under the ERH.

The redshift at the **red dot** is $z = 0.598$. By the standard formula the source would shine 5.9×10^9 years ago [19,20].

In this model, this source shone 1.37×10^{10} years ago.

The dent in the blue curve appears when the ray crosses the ERH on the other side of the center.



Nonradial rays propagating above the hump toward the same observer (left graph)

Along them, too, z is not monotonic (see right graph for ray 3).

The big dots are where the rays hit the last scattering hypersurface.

The present observer sees all these rays within a 2° cone around the central ray.

This angle may be made still smaller when the model is improved.

The presence of these rays makes the model falsifiable against observations.

A model of the whole Universe would consist of several L-T humps matched into the same Friedmann background.

Models of this type account for [18]:

- (1) The observed frequency range of the GRBs, $[0.24 \times 10^{19}, 1.25 \times 10^{23}]$ Hz;
- (2) Their limited duration (observed: up to 30 hours);
- (3) The afterglows (observed durations: up to several hundred days);
- (4) Their hypothetical collimation into narrow jets;
- (5) The large distances to their sources ($> 10^9$ ly);
- (6) The multitude of the observed GRBs (observed: a few each day, model says there are up to 10 300 potential sources in the whole sky at present. Whether this is enough or too few is not known).

Properties (2), (3) and (6) are accounted for only qualitatively (the effect is there, but the numbers do not agree with observations and the model needs improvements).

5. How would a shell crossing in an L-T model be seen by observers?

Light rays emitted at the Big Bang in an L-T model are seen by later observers either as infinitely redshifted, or as infinitely blueshifted.

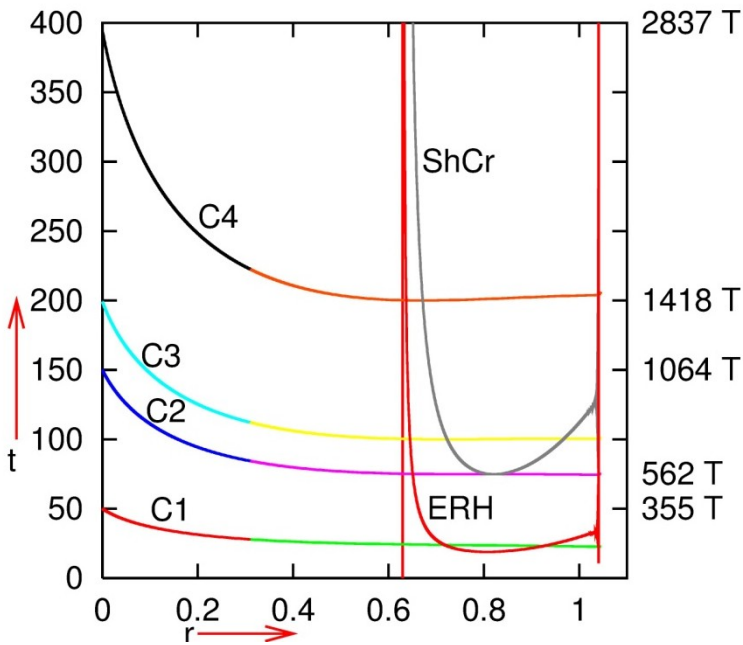
Does a shell crossing have any of these properties?

The answer was found as a by-product of investigation of another L-T model [21].

In this model a shell crossing would come into view of the central observer at ≈ 1000 \times the present age of the Universe to the future from now.

This investigation was done as an exercise in geometry, it is not cosmologically realistic.

[21] Kasiński 2014.



The configuration of the model

- $t = 0$ – the present time
- $T = 13.8 \times 10^9$ y – the present age of the Universe
- ShCr – the $t(r)$ profile of the shell crossing singularity
- ERH – the profile of the extremum redshift hypersurface
- C_1, \dots, C_4 – profiles of light cones at characteristic epochs

The model extends only up to $r \approx 1.05$.

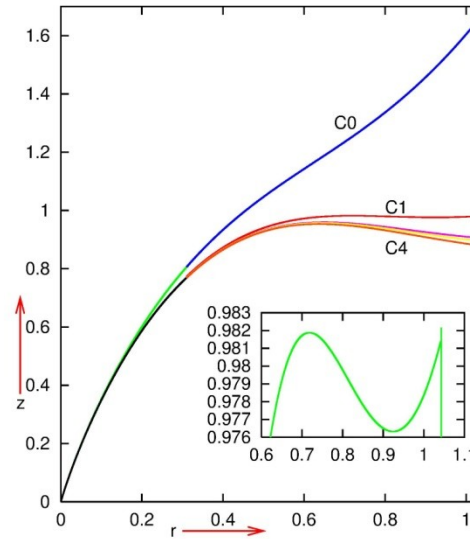
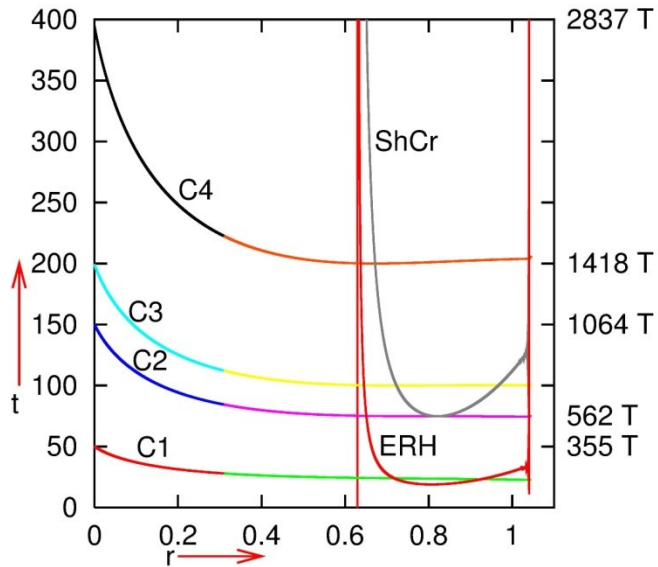
C_1 does not intersect the ShCr profile

C_2 is tangent to the ShCr profile at the minimum of $t(r)|_{\text{ShCr}}$

C_3 intersects the ShCr profile at two points

C_4 intersects the ShCr profile at one point

Surprise: the intersection of a ray with the ShCr leaves no trace in the $z(r)$ curve.



Along profiles that pass below the ERH (like C_0) $dz/dr > 0$ all the way.

On C_1 , which intersects the ERH twice, $z(r)$ has a maximum and a minimum – see inset.

On curves $C_2 - C_4$, $z(r)$ has a maximum, then decreases up to the edge of the model.

Nothing special happens with $z(r)$ at the intersections of the rays with the ShCr: the $z(r)$ curves are smooth and have no extrema there.

→ A shell-crossing would not be noticeable for an observer via $z(r)$.

In a neighbourhood of a shell crossing, $z(r)$ becomes nonmonotonic, and so fails to be a distance indicator, just like near a nonconstant t_B .

6. Expression of hope

Astronomers do not take the L-T models seriously, and do not welcome blueshifts.

In several papers blueshifts were argued to cause assorted disasters that disqualify these models.

My aim was to show that L-T models have interesting geometries, and that blueshifts imply interesting bits of optics.

History of science teaches us that if a well-tested theory predicts a phenomenon, then the prediction has to be taken seriously and verified experimentally.

Perhaps this will happen with the results reported here (but will it during our lifetime?).

7. References

- [1] F. J. Tipler, C. J. S. Clarke and G. F. R. Ellis, Singularities and Horizons -- a Review Article. In: *General Relativity and Gravitation. One Hundred Years After the Birth of Albert Einstein*, volume 2. Edited by A. Held. Plenum Press, New York 1980, p. 97.
- [2] J. M. M. Senovilla, Singularity Theorems and Their Consequences. *Gen. Relativ. Gravit.* **29**, 701 (1997).
- [3] H. P. Robertson, Relativistic cosmology, *Rev. Mod. Phys.* **5**, 62 (1933). Reprinted in *Gen. Relativ. Gravit.* **44**, 2115 (2012) with an editorial note by G. F. R. Ellis, p. 2099, and Robertson's brief biography by A. Krasinski, p. 2109.
- [4] A. G. Walker, On Riemannian spaces with spherical symmetry about a line, and the conditions for isotropy in general relativity, *Quart. J. Math. Oxford*, ser. 6, 81 (1935).

[5] A. A. Friedmann, Über die Krümmung des Raumes [On the curvature of space], *Z. Physik* **10**, 377 (1922); Über die Möglichkeit einer Welt mit konstanter negativer Krümmung des Raumes [On the possibility of a world with constant negative curvature of space], *Z. Physik* **21**, 326 (1924). English translations of both papers: *Gen. Relativ. Gravit.* **31**, 1991 and 2001 (1999) with an editorial note by A. Krasinski and G. F. R. Ellis, p. 1985, and Friedmann's brief biography by A. Krasinski, p. 1989. See also the addendum: *Gen. Relativ. Gravit.* **32**, 1937 (2000).

[6] V. A. Ruban, T-modeli `shara' v obshchey teorii otnositelnosti [T-models of a `sphere' in general relativity theory], *Pis'ma v Red. ZhETF* **8**, 669 (1968). English translation: *Sov. Phys. JETP Lett.* **8**, 414 (1968).

[7] V. A. Ruban, Sfericheski-symmetrichnye T-modeli v obshchey teorii otnositelnosti [Spherically symmetric T-models in the general theory of relativity], *Zh. Eksper. Teor. Fiz.* **56**, 1914 (1969). English translation: *Sov. Phys. JETP* **29**, 1027 (1969).

English translations of both papers by Ruban reprinted in *Gen. Relativ. Gravit.* **33**, 369 and 375 (2001), with an editorial note by A. Krasinski, p. 363 and Ruban's brief biography by I. Dymnikova, p. 366.

[8] C. Hellaby and K. Lake, Shell crossings and the Tolman model, *Astrophys. J.* **290**, 381 (1985) + erratum *Astrophys. J.* **300**, 461 (1985).

[9] G. Lemaître, L'Univers en expansion [The expanding Universe], *Ann. Soc. Sci. Bruxelles* **A53**, 51 (1933). English translation: *Gen. Relativ. Gravit.* **29**, 641 (1997), with an editorial note and a brief biography of Lemaître by A. Krasinski, p. 637.

[10] R. C. Tolman, Effect of inhomogeneity on cosmological models, *Proc. Nat. Acad. Sci. USA* **20**, 169 (1934). Reprinted in *Gen. Relativ. Gravit.* **29**, 935 (1997), with an editorial note and a brief biography of Tolman by A. Krasinski, p. 931.

[11] H. Bondi, Spherically symmetrical models in general relativity. *Mon. Not. Roy. Astr. Soc.* **107**, 410 (1947). Reprinted in *Gen. Relativ. Gravit.* **31**, 1783 (1999), with an editorial note by A. Krasinski, p. 1777, and a brief autobiography by Bondi, p. 1780.

[12] Planck collaboration, Planck 2013 results. XVI. Cosmological parameters. *Astronomy and Astrophysics* **571**, A16 (2014).

[13] H. Iguchi, T. Nakamura and K. Nakao, Is dark energy the only solution to the apparent acceleration of the present Universe? *Progr. Theor. Phys.* **108**, 809 (2002).

- [14] C.-M. Yoo, T. Kai, K-i. Nakao, Solving the inverse problem with inhomogeneous universes. *Progr. Theor. Phys.* **120**, 937 (2008).
- [15] A. Krasinski, Accelerating expansion or inhomogeneity? A comparison of the Λ CDM and Lemaître -- Tolman models. *Phys. Rev.* **D89**, 023520 (2014); erratum: *Phys. Rev.* **D89**, 089901(E) (2014).
- [16] A. Krasinski, Accelerating expansion or inhomogeneity? Part 2: Mimicking acceleration with the energy function in the Lemaître -- Tolman model. *Phys. Rev.* **D90**, 023524 (2014).
- [17] <http://astronomy.swin.edu.au/cosmos/e/epoch+of+recombination>
- [18] A. Krasinski, Cosmological blueshifting may explain the gamma ray bursts. *Phys. Rev.* **D93**, 043525 (2016).
- [19] E. L. Wright, A Cosmology Calculator for the World Wide Web. *Publ. Astr. Soc. Pac.* **118**, 1711 (2006).
- [20] E. L. Wright, <http://www.astro.ucla.edu/~wright/ACC.html>

- [21] A. Krasinski, Mimicking acceleration in the constant-bang-time Lemaître -- Tolman model: Shell crossings, density distributions and light cones. *Phys. Rev.* **D90**, 064021 (2014).
- [22] P. Szekeres, A class of inhomogeneous cosmological models. *Commun. Math. Phys.* **41**, 55 (1975).
- [23] A. Krasinski, Existence of blueshifts in quasi-spherical Szekeres spacetimes. arXiv:1604.02003, submitted for publication.

Appendix: 8. The quasi-spherical Szekeres models

The quasi-spherical Szekeres solutions [22] have the metric

$$\begin{aligned} ds^2 &= dt^2 - \frac{\mathcal{E}^2(\Phi/\mathcal{E})_{,r}{}^2}{1 + 2E(r)} dr^2 - \frac{\Phi^2}{\mathcal{E}^2} (dx^2 + dy^2), \\ \mathcal{E} &\stackrel{\text{def}}{=} \frac{(x - P)^2}{2S} + \frac{(y - Q)^2}{2S} + \frac{S}{2}, \end{aligned} \quad (8.1)$$

where $E(r)$, $M(r)$, $P(r)$, $Q(r)$ and $S(r)$ are arbitrary functions, and

$$\Phi_{,t}{}^2 = 2E(r) + \frac{2M(r)}{\Phi} + \frac{1}{3}\Lambda\Phi^2. \quad (8.2)$$

The mass density is

$$\kappa\rho = \frac{2(M/\mathcal{E}^3)_{,r}}{(\Phi/\mathcal{E})^2(\Phi/\mathcal{E})_{,r}}, \quad \kappa = \frac{8\pi G}{c^2}. \quad (8.3)$$

Eq. (8.2) is the same as in the L-T model, and, as before, implies that the bang time is in general position-dependent:

$$\int_0^{\Phi} \frac{d\tilde{\Phi}}{\sqrt{2E + 2M/\tilde{\Phi} + \frac{1}{3}\Lambda\tilde{\Phi}^2}} = t - t_B(r). \quad (8.4)$$

$$ds^2 = dt^2 - \frac{\mathcal{E}^2(\Phi/\mathcal{E})_{,r}{}^2}{1 + 2E(r)} dr^2 - \frac{\Phi^2}{\mathcal{E}^2} (dx^2 + dy^2), \quad \mathcal{E} = \frac{(x - P)^2}{2S} + \frac{(y - Q)^2}{2S} + \frac{S}{2}, \quad (8.1)$$

$$\Phi_{,t}{}^2 = 2E(r) + \frac{2M(r)}{\Phi} + \frac{1}{3}\Lambda\Phi^2, \quad (8.2)$$

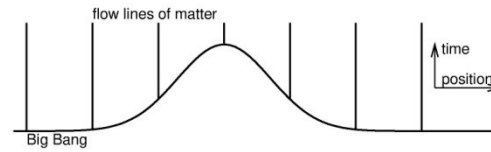
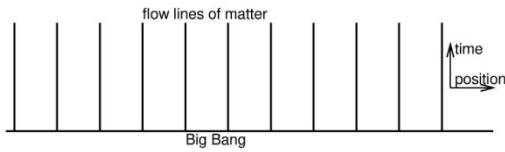
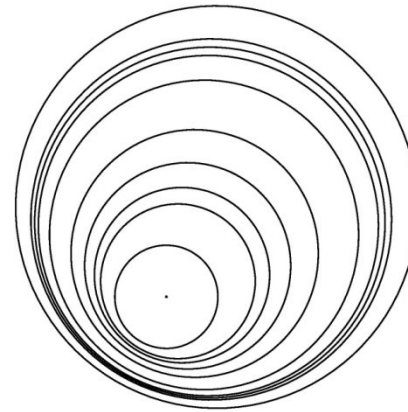
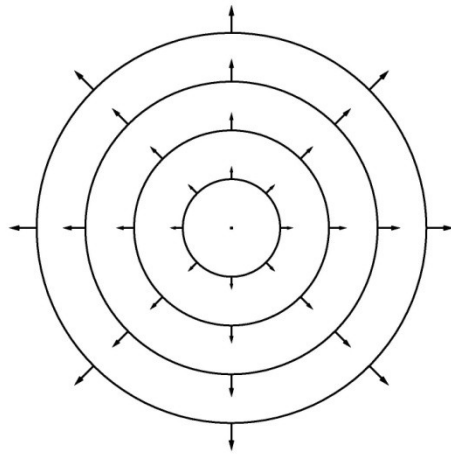
$$\int_0^\Phi \frac{d\tilde{\Phi}}{\sqrt{2E + 2M/\tilde{\Phi} + \frac{1}{3}\Lambda\tilde{\Phi}^2}} = t - t_B(r). \quad (8.4)$$

The source in the Einstein equations is dust.

A general Szekeres metric has no symmetry. The surfaces of constant t and r are **nonconcentric spheres**, x and y are stereographic coordinates on the spheres.

The L-T model is contained here as the limit of constant (P, Q, S) – then the spheres become concentric.

The Friedmann limit follows when, in addition, $\phi(t,r) = rR(t)$, $2E = -kr^2$ where $k = \text{const}$ is the Friedmann curvature index and t_B is constant.



A comparison of the expansion patterns in the R-W models (left) and in the quasi-spherical Szekeres models (right).

9. Blueshifts in quasi-spherical Szekeres models

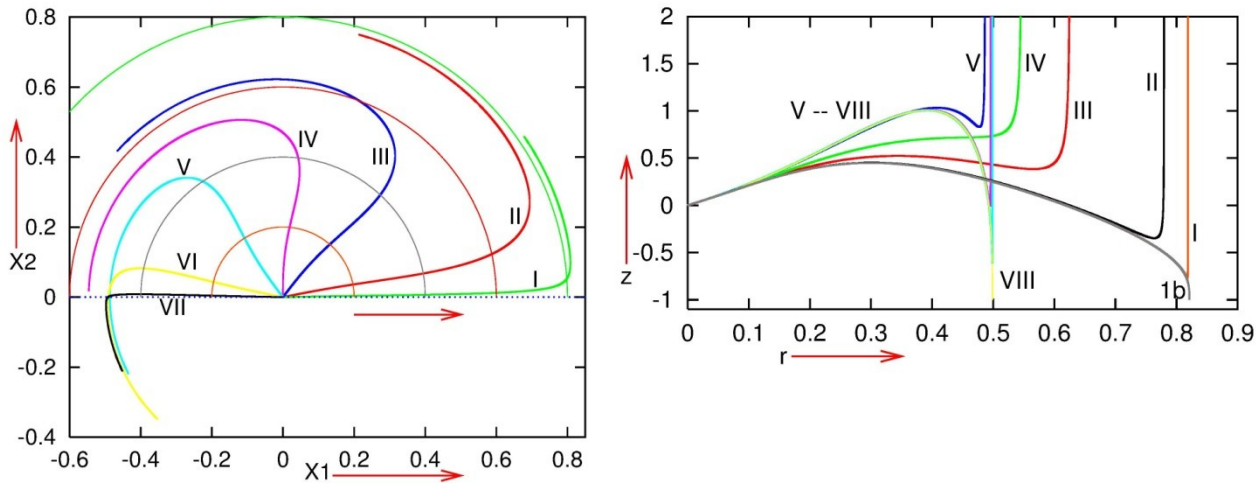
In L-T models, blueshifts may appear only on radial rays.

But when the spacetime has no symmetry, no radial directions exist. Can blueshifts appear in the Szekeres models?

When a quasi-spherical Szekeres model is *axially* symmetric, infinite blueshifts can possibly appear *only* on such rays that intersect every space of constant t on the symmetry axis [23]; call them *axial rays* (this is an exact result).

Numerical calculations confirm that strong blueshifts indeed appear on axial rays emitted at a nonconstant BB [23].

In a nonsymmetric Szekeres model, numerical calculations show that two opposite directions exist, along which strong blueshifts are generated [23].



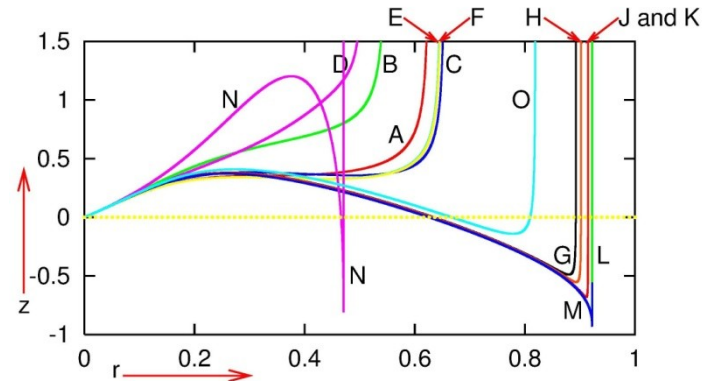
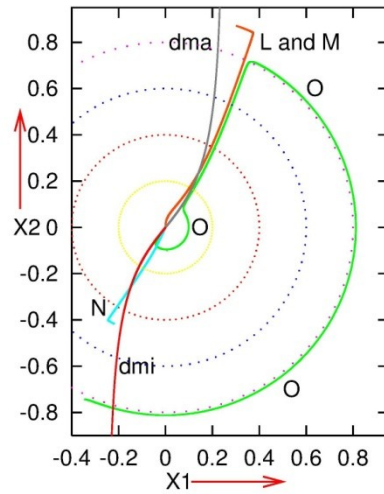
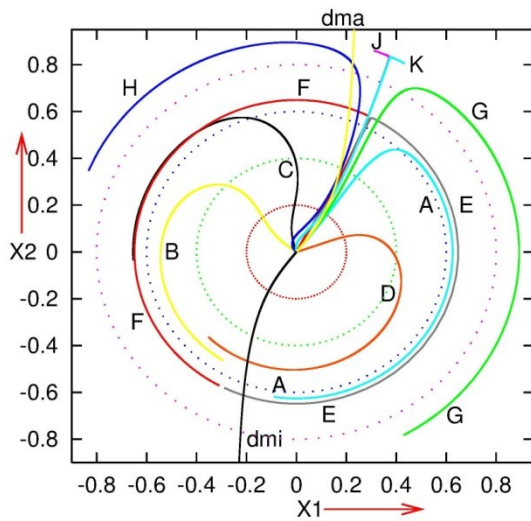
The polar graphs of selected rays (left) and the redshift profiles along them (right) in an axially symmetric quasi-spherical Szekeres model

The coordinates of the graph at left are $X_1 = r \cos \varphi$ and $X_2 = r \sin \varphi$.

The line $X_2 = 0$ is the projection of the axial rays.

Minimum z becomes near to -1 when the direction of the ray approaches axial; on the axial rays 1b and VIII, $1 + z < 10^{-5}$.

Nonaxial rays hit the BB being tangent to $r = \text{constant}$ surfaces, with $z \rightarrow \infty$ (the same happens in L-T with nonradial rays).



The polar graphs of exemplary rays (left and center) and the redshift profiles along them (right) in a nonsymmetric quasi-spherical Szekeres model

The graphs show similar patterns to those in the axially symmetric case.

There clearly exist preferred null curves in a general Szekeres model, but their interpretation is unknown.

They *do not* coincide with the two principal null directions of the Weyl tensor [23] (the Szekeres metrics are of type D).